Medicinal Chemistry Research
https://doi.org/10.1007/s00044-020-02589-2

MEDICINAL CHEMISTRY RESEARCH

ORIGINAL RESEARCH

Design, synthesis and biological evaluation of novel indolinedione–coumarin hybrids as xanthine oxidase inhibitors

Harmandeep Kaur Gulati[1] · Kavita Bhagat[1] · Atamjit Singh[1] · Nitish Kumar[1] · Arshmeet Kaur[1] · Akriti Sharma[1] · Shilpa Heer[1] · Harbinder Singh[1] · Jatinder Vir Singh[1] · Preet Mohinder S. Bedi[1]

Received: 21 January 2020 / Accepted: 8 June 2020

Abstract

A library of indolinedione–coumarin hybrid molecules was rationally designed and synthesized against hyperuricemia. All of the synthesized hybrid molecules were tested to check their inhibitory activity against xanthine oxidase enzyme by using a spectrophotometric assay. The results revealed that the compound showed IC_{50} values within the range of 6.5–24.5 µM amongst which compound **K-7** was found to be endowed with the most potent IC_{50} value against xanthine oxidase enzyme. Kinetic studies were also performed to check the mode of inhibition of most potent compound **K-7**, which revealed its mixed-type inhibition behavior. Structure-activity relationships revealed that electron-donating groups and small alkyl chains between the two active scaffolds might be beneficial in inhibiting xanthine oxidase enzyme. It was also shown that various electrostatic interactions stabilized the compound **K-7** within the active site of xanthine oxidase enzyme, which confirmed that it can completely block its catalytic active site. Thus, **K-7** is regarded as a potent xanthine oxidase inhibitor and can be served as a promising molecular architectural unit for anti-hyperuricemic drug design.

Graphical Abstract

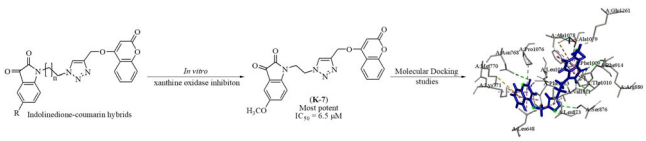

Keywords Indolinedione · Coumarin · Hybrids · Xanthine oxidase enzyme · Enzyme kinetics · Molecular docking studies

Introduction

Xanthine oxidase (XO), a molybdoflavoprotein containing iron and molybdenum, that promotes the oxidation, especially of hypoxanthine to xanthine and then to uric acid (UA) with the release of hydrogen peroxide and superoxide anions during the process of purines catabolism in humans. A well-known relationship exists between XO and hyperuricemia, a condition which is characterized by elevated serum UA level (7 mg/dL) (Wortmann 1998). Impairment in purine metabolism results in the deposition of sodium urate crystals in joints, which further causes inflammation and pain in joints. With this aspect, XO acts as an important and selective target for sustaining broad-spectrum chemotherapy in hyperuricemic patients (Ojha et al. 2017; Kumar et al. 2011).

Supplementary information The online version of this article (https://doi.org/10.1007/s00044-020-02589-2) contains supplementary material, which is available to authorized users.

✉ Harbinder Singh
singh.harbinder40@gmail.com

✉ Jatinder Vir Singh
jatindervirsingh1@gmail.com

✉ Preet Mohinder S. Bedi
bedi_preet@yahoo.com

[1] Department of Pharmaceutical Sciences, Guru Nanak Dev University, Amritsar, Punjab 143005, India

Published online: 16 June 2020

In the recent past, numerous successful purine based XO inhibitors such as allopurinol, pterin and 6-formylpterin (Oettl and Reibneggar 1999), 2-alkylhypoxanthines (Oettl and Reibneggar 1999; Biagi et al. 2001; Brien et al. 1985), and 2-substituted 7Hpyrazolo-[4,3-e]-1,2,4-triazolo-[1,5-c]-pyrimidines (Nagamatsu et al. 2000; Nagamatsu et al. 1985; Nagamatsu et al. 1995; Ali et al. 2010) are used for the treatment of hyperuricemia. These derivatives were mainly associated with the number of side effects (Stevens–Johnson syndrome and drug rash with eosinophilia and systematic symptoms (Ali et al. 2010; Pacher et al. 2006; Hille 2006) and also hindered the activities of both purine and pyrimidine metabolizing enzymes, which motivate the researchers around the globe to develop non-purine XO inhibitors (Pacher et al. 2006; Hille 2006; Borges et al. 2002).

Therefore, researchers paid great attention to the development of non-purine XO inhibitors. The compound BOF-4272, a potent XO inhibitor, its clinical use was limited because variation occurring in its efficacy which is mainly due to the difference in hepatic metabolism (Pacher et al. 2006). Febuxostat, a non-purine XO inhibitor that was approved from European Medicines Evaluation Agency and USFDA showed efficient efficacy with improved hypouricemic effect as compared with Allopurinol (Osada et al. 1993; Komoriya et al. 1993; Becker et al. 2004). Besides this, it was also reported that Febuxostat showed some side effects similar to Allopurinol such as headache, diarrhea, dizziness, abnormalities in liver function, and nausea (Strilchuk et al. 2019; Love et al. 2010; Becker et al. 2007; Schumacher et al. 2008; Becker et al. 2007). Furthermore, pyranostat was found to show higher in vivo efficacy with a poor pharmacokinetic profile (Ishibuchi et al. 2001; Sebastian et al. 2016). Whereas, topiroxostat, another non-purine based XO inhibitor, was also showed significant activity but with similar side effects as allopurinol (Pascart and Richette 2018). Based on these particular results, it can be concluded that researchers that involved in this field must develop alternate scaffolds that act as potent XO inhibitors with lesser side effects that can be used for the treatment of hyperuricemia.

Besides these, many researchers have also focussed on XO inhibitors derived from natural compounds-flavonoids, hydroxycinnamic acids, tannins, chalcones, saponins, terpenoids, stilbenes, phenylethanoid glycosides, since these can act as lead compounds for the discovery of new synthetics (Malik et al. 2018; Mehmood et al. 2019).

Coumarin is a natural moiety that is known to its various biological activities, also found to be a potent XO inhibitor. Numerous reports on the XO inhibitory potential of coumarin derivatives are available (Fais et al. 2018; Chen et al. 2014). Figure 1 depicts recently reported coumarin derivatives with XO inhibitory potential. Therefore, it could be an ideal moiety to be included in the novel alternative molecular architecture for the further development of XO inhibitors.

From the last 5 years, we are continuously working on the similar lines to develop non-purine based XO inhibitors (Dhiman et al. 2012; Shukla et al. 2014; Sharma et al. 2014; Virdi et al. 2014; Kaur et al. 2015; Kaur et al. 2015, Kaur et al. 2017; Singh et al. 2019; Kaur et al. 2019) and now, we have come up with a new series of coumarin hybrid molecules clubbed with indolinedione with the help of triazole moiety as a linker. The rationale for the inclusion of indolinedione to the designed molecules is very clear. The two carbonyl groups and the nitrogen atom of the indole ring could act as hydrogen bond acceptor in the active site of the XO enzyme, which was confirmed through molecular modeling studies in the current evaluation. 1,2,3-triazole is also an active moiety owing to its three H-bond acceptor-Nitrogen atoms, the inclusion of which could also be beneficial for its better interactions within the XO enzyme.

Results and discussion

Indolinedione–coumarin hybrids were synthesized by following the synthetic Scheme 1. At first, substituted indolinediones were stirred with 1,2-dibromoalkanes (1 eq) at room temperature using Dimethylformamide (DMF) as a solvent, and potassium carbonate (1.5 eq) as a base. The resulting product was then dissolved in DMF and then sodium azide (1 eq) was added. The reaction mixture was stirred at room temperature to form 1-(4-azidoalkyl)indoline-2,3-diones.

Then, 4-hydroxycoumarin and propargyl bromide (1.2 eq) were stirred in DMF under basic conditions (K_2CO_3; 1.5 eq) to obtain 4(prop-2-ynyloxy)-2H-chromen-2-one (PHC).

This 4-(prop-2-ynyloxy)-2H-chromen-2-one (PHC) was further reacted with various 1-(4-azidoalkyl)indoline-2,3-dione analogues in the presence of pentahydrate $CuSO_4$ (catalytic amount) and sodium ascorbate (as a reducing agent of $CuSO_4$), in DMF at room temperature to obtain the desired hybrid compounds. All compounds were monitored by thin-layer chromatography in the reaction, purified by column chromatography. ^{1}H NMR and ^{13}C NMR spectroscopic techniques were used to characterize the synthesized compounds and all the spectral data was found in accordance with assumed structures.

In vitro xanthine oxidase assay

All the synthesized compounds were evaluated to test their inhibition against XO enzyme at five different concentrations ranging from 1 to 50 μM. The formation of UA was determined by using UV spectrophotometer at 292 nm and

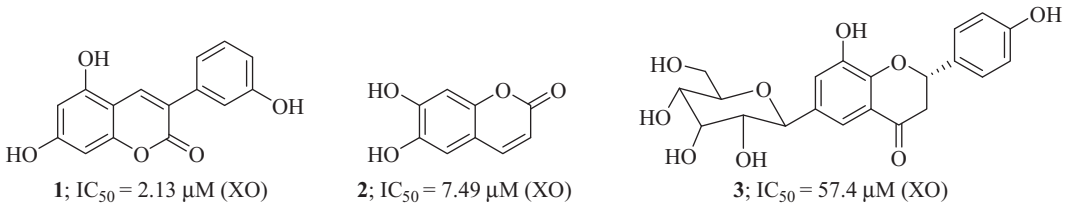

Fig. 1 Recently reported potent coumarin derivatives as XO inhibitors

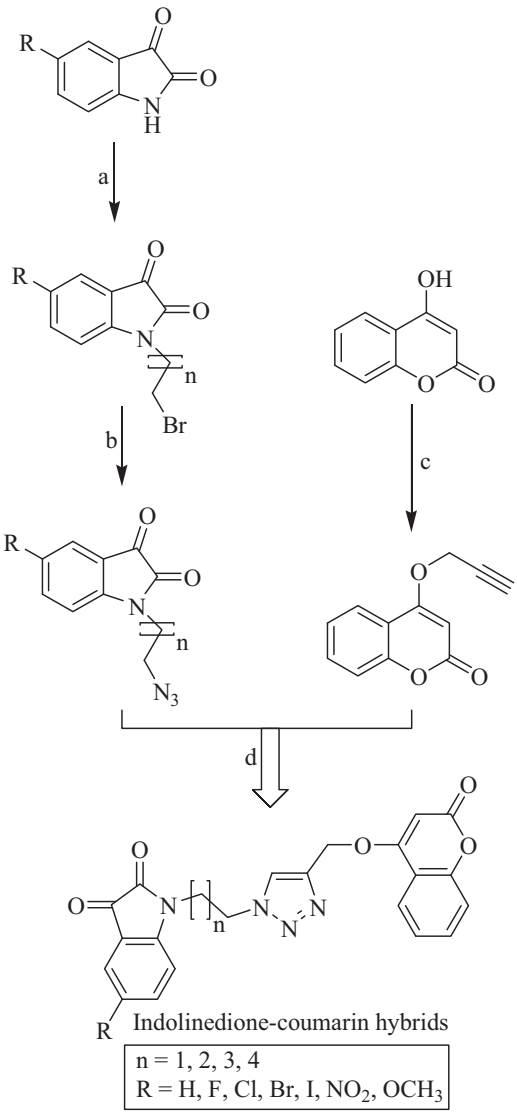

Scheme 1 Synthesis of indolinedione–coumarin hybrids. Reagents and conditions: (**a**) dibromoalkanes, K_2CO_3, DMF, 2 h, stir, rt; (**b**) NaN_3, DMF, 1 hr, stir, rt; (**c**) Propargyl bromide, K_2CO_3, DMF, 2 h, stir, rt; (**d**) Sodium ascorbate, $CuSO_4$, DMF, 15 min, rt

Code	n	R
K-1	1	H
K-2	1	F
K-3	1	Cl
K-4	1	Br
K-5	1	I
K-6	1	NO_2
K-7	1	OCH_3

Code	n	R
L-1	2	H
L-2	2	F
L-3	2	Cl
L-4	2	Br
L-5	2	I
L-6	2	NO_2
L-7	2	OCH_3

Code	n	R
M-1	3	H
M-2	3	F
M-3	3	Cl
M-4	3	Br
M-5	3	I
M-6	3	NO_2
M-7	3	OCH_3

percentage inhibition was calculated for each compound. (Table 1). The results of the assay revealed that compounds showed good to moderate inhibition. Two compounds (**K-1** & **K-7**) showed above 80% inhibition against the enzyme at 50 μM concentration, while some displayed below 30% inhibition even at 50 μM concentration. The concentration at which 50% of the enzyme was inhibited, was calculated only for those compounds which inhibited the enzyme above 50% at 50 μM concentration. Two compounds (**K-1** & **K-7)** were found to be endowed with the most prominent inhibition with the IC_{50} values of 8.9 μM and 6.5 μM, respectively. The IC_{50} values of all the compounds were ranging from 6.5 to 24.5 μM. The results revealed that the structural architecture of the compounds greatly influences the inhibitory activity. For instance, the compounds bearing electron-donating groups (-OCH_3) on 5th position of

Table 1 Xanthine oxidase inhibitory activity of all the synthesized compounds

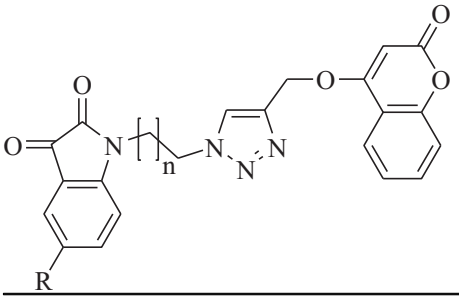

Compound	*R*	*n*	Percent inhibition					IC_{50} (μM)
			1 (μM)	5 (μM)	10 (μM)	25 (μM)	50 (μM)	
K-1	H	1	32	42	62	79	85	8.9 ± 0.12
K-2	F	1	20	29	39	52	57	18.4 ± 1.9
K-3	Cl	1	24	30	40	56	61	15.6 ± 1.43
K-4	Br	1	23	34	45	60	65	14.3 ± 1.23
K-5	I	1	23	39	48	59	70	11.4 ± 1.08
K-6	NO_2	1	21	30	38	53	59	12.5 ± 1.09
K-7	OCH_3	1	35	49	69	85	92	6.5 ± 0.09
L-1	H	2	25	29	41	57	63	15.7 ± 1.45
L-2	F	2	12	19	25	34	45	–
L-3	Cl	2	11	17	28	39	49	–
L-4	Br	2	19	28	34	51	57	24.5 ± 2.87
L-5	I	2	21	30	40	53	60	17.8 ± 1.98
L-6	NO_2	2	10	17	26	32	44	–
L-7	OCH_3	2	23	40	49	60	69	12.4 ± 0.98
M-1	H	3	9	15	21	30	44	–
M-2	F	3	3	5	9	18	30	–
M-3	Cl	3	4	8	13	22	38	–
M-4	Br	3	8	14	20	27	39	–
M-5	I	3	7	13	21	28	41	–
M-6	NO_2	3	2	8	17	24	29	–
M-7	OCH_3	3	19	30	37	51	55	20 ± 1.76
Allopurinol								8.16 ± 1.27

indolinedione moiety enhanced the activity as compared with the compounds bearing electron-withdrawing groups (halogen atoms). The chain length between indolinedione and triazole moieties also affects the activity, as the chain length increases the inhibitory activity gradually decreases. Therefore, the activity order for substitution on 5th position of indolinedione followed as: -OCH_3 > H > I > Br > Cl > F ≈ NO_2 and for chain length (*n*): 1 > 2 > 3. From these results, it has been cleared that relatively compounds with high molecular weight are less potent than that of small molecules. This can be explained on the basis of the size of the active pocket of the enzyme XO, which is relatively very small and those compounds which can well occupy in the cavity showed the inhibitory activity (Table 1). This was also confirmed through molecular modeling studies in section (Molecular modelling studies).

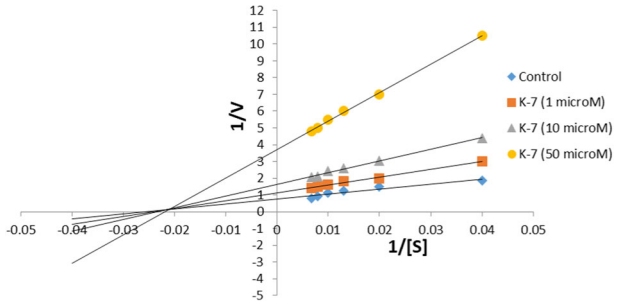

Fig. 2 Lineweaver–Burk plot of **K-7**

Enzyme kinetics

Compound **K-7** was further investigated for the type of inhibition by performing enzyme kinetic studies (Fig. 2). The pattern of the Lineweaver–Burk plot graph shows that

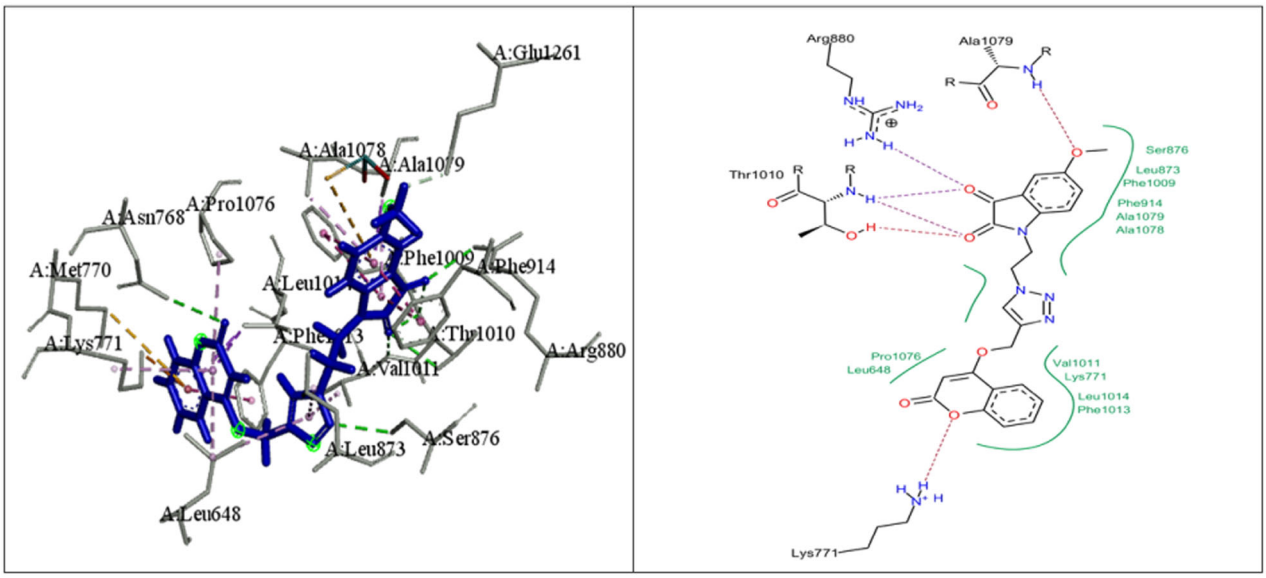

Fig. 3 3D representation of **K-7** (blue) within the active site of XO enzyme (Left-hand side), 2D representation of **K-7** within the active site of the enzyme (right-hand side)

it is a form of mixed inhibition scenario where K_m, V_{max}, and slope are all affected by the inhibitor. The inhibitor has increased the K_m and slope (K_m/V_{max}) while decreasing the V_{max}. Moreover, on careful observation, it was found that intersecting lines on the graph converge to the left of the y-axis and above the x-axis which indicates that the value of α (a constant that defines the degree to which inhibitor binding affects the affinity of the enzyme for substrate) is >1 (Copeland 2005). This confirms that the inhibitor preferentially binds to the free enzyme and not the enzyme-substrate complex. Therefore, the mode of inhibition of **K-7** is mixed-type but it seems that it has a strong competitive component.

Molecular modeling studies

Molecular modeling studies were performed to elucidate interactions of the most potent compound **K-7** within the active site of XO enzyme. The X-ray crystallographic structure of XO, complexed with febuxostat (PDB entry: 1N5X; resolution 2.8 Å) was employed. The accuracy of the docking program was validated by docking co-crystallized ligand febuxostat in its binding pocket. The program was able to reproduce best fit confirmation of febuxostat with a root mean square deviation of 0.523 indicating the reliability of docking protocol. After that, compound **K-7** was docked into febuxostat binding site and its top best pose with dock score of −32.2563 was selected for discussion (Fig. 3).

Overall binding mode of compound **K-7** with residues of the binding site suggests that compound fits well in the cavity and is well stabilized by various electrostatic interactions. Major interactions with XO enzyme include π-sigma, π-alkyl, carbon-hydrogen bond, π-donor hydrogen bond, and conventional hydrogen bond interaction. Indolinedione moiety is well positioned in a cavity formed by hydrophobic residues Ser876, Leu873, Phe1009, Phe914, Ala1079, and Ala1078. The methoxy group present on the 5th position of indolinedione forms the conventional hydrogen bond with the amine group of Ala1079. Three additional hydrogen bonds are formed as expected with the two carbonyl groups of indolinedione with amino acid residues Arg880 and Thr1010. On the other end, coumarin moiety is inserted into the cavity formed by various hydrophobic amino acids Pro1076, Leu648, Val1011, Lys771, Leu1014, and Phe1013 and also stabilized by H-bond interaction with Lys771 through an oxygen atom of pyran ring (Fig. 3). Therefore, docking studies suggest that the **K-7** completely blocks the binding pocket of the XO enzyme to exert its inhibitory action which also supports its potent in vitro activity.

Conclusion

Coumarin and indolinedione are multifunctional products and in the current study, we have rationally designed and synthesized various Indolinedione–coumarin molecular hybrids. Their bioactivities were evaluated in terms of their XO inhibitory potential. Almost all of the compounds were found active while two compounds **K-1** and **K-7** showed better results in vitro and were potent ones as compared

with standard drug allopurinol. Structure-activity relationship revealed that the compounds with electron-donating groups (-OCH_3) increased the activity and length of two carbon chain between indolinedione and triazole moieties are most favorable, one for the inhibitory potential. Kinetic studies indicated that **K-7** showed its mixed-type inhibition scenario against the XO enzyme. Various binding interactions of **K-7** with the active site of the XO enzyme were also streamlined by using docking studies. Therefore, these compounds could act as hit lead molecules for the further development of potent XO inhibitors.

Experimental

Material and measurements

The chemical reagents were procured from CDH, Sigma-Aldrich, and Loba, India. All yields refer to isolated products after purification. Products were characterized by comparing with authentic samples and by spectroscopic techniques i.e., ^{1}H and ^{13}C NMR, Elemental Analysis). Avance III HD 500 MHz Bruker Biospin and JEOL AL 300 MHz machines were used to record the NMR spectra. The spectra were recorded by dissolving in $CDCl_3$ and DMSO-d_6 relative to TMS (0.00 ppm). In ^{1}H NMR chemical shifts were reported in δ values using an internal standard (tetramethylsilane) with a number of protons, multiplicities (s-singlet, d-doublet, t-triplet, q-quartet, m-multiplet) and coupling constants (J) in Hertz (Hz). Melting points were determined in open capillaries and were uncorrected.

General procedure for the synthesis of 4-(prop-2-ynyloxy)-2H-chromen-2-one (PGC)

In 50 mL of DMF, 4-Hydroxy coumarin (20 g) was dissolved with the addition of propargyl bromide (1.2 eq) and K_2CO_3 (1.5 eq). The reaction mixture was stirred at room temperature and the reaction was continuously monitored by TLC. After the completion of the reaction, the reaction mixture was poured on crushed ice. The solid product of propargylated coumarin thus obtained was filtered, washed with cold water, and air-dried. The physical data of propargylated coumarin is given below:

4-(prop-2-ynyloxy)-2H-chromen-2-one (PGC)

Yield 80%; mp 103–107 °C.^{1}H NMR ($CDCl_3$, 500 MHz, δ, TMS = 0): 3.22–3.24 (m, 1H, -CH-propargylic), 4.92–4.94 (m, 2H, -CH_2-), 5.84 (d, 1H, J = 12 Hz, -CH-), 7.25–7.27 (m, 2H, ArH), 7.56 (s, 1H, ArH), 7.77 (d, 1H, J = 8 Hz, ArH). ^{13}C NMR ($CDCl_3$, 125 MHz, δ, TMS = 0): 57.38, 76.50, 79.32, 91.71, 115.39, 116.60, 123.16, 124.28, 132.83, 153.17, 162.02, 164.24.

General procedure for the synthesis of 1-(2-bromoalkyl) indoline-2,3-diones

Indoline-2,3-dione (1 eq) was dissolved in DMF (in minimum amount), dibromoalkane (1 eq) and K_2CO_3 (1.5 eq) were added. The reaction mixture was stirred at room temperature. After the completion of the reaction as confirmed by TLC, the reaction mixture was poured on crushed ice. The impure product so obtained was filtered, air-dried, and subjected to column chromatography (hexane/ethyl acetate as eluent) to gain the desired product. All the other 1-bromoalkylindoline-2,3-diones were synthesized via the same procedure as mentioned above using various dibromoalkanes.

General procedure for the synthesis of 1-(4-azidoalkyl) indoline-2,3-diones (IBA)

In a minimum amount of DMF, 1-(4-Bromoalkyl)indoline-2,3-dione (1 eq) were dissolved and sodium azide (1 eq) was added and the mixture was stirred at room temperature. After the completion of the reaction, the reaction mixture was poured on crushed ice and precipitates (1-(4-azidoalkyl)indoline-2,3-diones) thus obtained were collected by simple filtration.

All the other 1-azidoalkylindoline-2,3-dione analogues were synthesized by following the above-mentioned procedure.

General procedure for the synthesis of triazole linked indoline-2,3-dione-coumarin hybrids

In DMF, 1-azidoalkylindoline-2,3-dione(1 eq) and 4-(prop-2-ynyloxy)-2H-chromen-2-one (PHC) (1 eq) were dissolved. The catalytic amount of pentahydrate copper sulphate ($CuSO_4.5H_2O$) and its reducing agent, sodium ascorbate were added in it. Reaction mixture was kept aside for some time, at room temperature. After the completion of reaction as confirmed by TLC, the reaction mixture was filtered directly on crushed ice to remove the excess of $CuSO_4$ and sodium ascorbate. The solidified final product thus obtained was filtered and air-dried. The physical data of all the synthesized bi-functional hybrids is given below:

1-(2-(4-((2-oxo-2H-chromen-4-yloxy)methyl)-1H-1,2,3-triazol-1-yl)ethyl)indoline-2,3-dione (K-1): Yield 78%, mp 104–108 °C. ^{1}H NMR (d$_6$-DMSO, 300 MHz, δ, TMS = 0): 4.21 (s, 2H, -CH_2-), 4.77 (s, 2H, -CH_2-), 5.38 (s, 2H, -CH_2-), 6.11 (s, 1H, -CH-), 6.91 (d, 1H, J = 7.8 Hz, ArH), 7.08 (t, 1H, ArH, J = 7.5 Hz), 7.41–7.46 (m, 2H, ArH), 7.54–7.56

(m, 2H, ArH), 7.68–7.71 (m, 2H, ArH), 8.49 (s, 1H, ArH). ^{13}C NMR (d_6-DMSO, 125 MHz, δ, TMS = 0): 47.64, 62.93, 91.50, 110.52, 115.43, 116.84, 117.64, 123.29, 123.79, 124.64, 125.00, 133.33, 138.59, 150.54, 153.11, 158.55, 162.14, 164.73, 183.32. Anal.Calcd for $C_{22}H_{16}N_4O_5$: C, 63.46; H, 3.87; N, 13.46 Found: C, 63.26; H, 3.98; N, 13.15.

1-(2-(4-((2-oxo-2H-chromen-4-yloxy)methyl)-1H-1,2,3-triazol-1-yl)ethyl)-5-fluoroindoline-2,3-dione (K-2): Yield 79%, mp 74–78 °C. ^{1}H NMR (d_6-DMSO, 300 MHz, δ, TMS = 0): 4.22 (s, 2H, -CH_2-), 4.76 (s, 2H, -CH_2-), 5.39 (s, 2H, -CH_2-), 6.14 (s, 1H, -CH-), 6.94 (s, 1H, ArH), 7.40–7.47 (m, 4H, ArH), 7.69–7.71 (m, 2H, ArH), 8.51 (s, 1H, ArH). ^{13}C NMR (d_6-DMSO, 125 MHz, δ, TMS = 0): 47.61, 63.06, 79.06, 79.32, 79.58, 91.60, 111.80, 112.00, 112.07, 115.45, 116.87, 118.58, 118.64, 123.22, 124.60, 133.28, 146.86, 153.16, 158.59, 162.03, 164.72, 182.73. Anal.Calcd for $C_{22}H_{15}FN_4O_5$: C, 60.83; H, 3.48; F, 4.37; N, 12.90 Found: C, 60.52; H, 3.50; F, 4.21; N, 12.96.

1-(2-(4-((2-oxo-2H-chromen-4-yloxy)methyl)-1H-1,2,3-triazol-1-yl)ethyl)-5-chloroindoline-2,3-dione (K-3): Yield 79%, mp 160–164 °C. ^{1}H NMR (d_6-DMSO, 500 MHz, δ, TMS = 0): 4.16 (s, 2H, -CH_2-), 4.70 (s, 2H, -CH_2-), 5.34 (s, 2H, -CH_2-), 6.09 (s, 1H, -CH-), 6.88 (d, 1H, J = 8.5 Hz, ArH), 7.35–7.40 (m, 2H, ArH), 7.56–7.57 (m, 2H, ArH), 7.64–7.67 (m, 2H, ArH), 8.45 (s, 1H, ArH). ^{13}C NMR (d_6-DMSO, 125 MHz, δ, TMS = 0): 47.59, 63.15, 91.68, 112.35, 115.49, 116.90, 119.13, 123.23, 124.48, 124.66, 126.67, 128.02, 133.26, 137.35, 149.19, 153.20, 158.34, 161.99, 164.74, 182.25. Anal.Calcd for $C_{22}H_{15}ClN_4O_5$: C, 58.61; H, 3.35; Cl, 7.86; N, 12.43 Found: C, 58.33; H, 3.54; Cl, 7.77; N, 12.55.

1-(2-(4-((2-oxo-2H-chromen-4-yloxy)methyl)-1H-1,2,3-triazol-1-yl)ethyl)-5-bromoindoline-2,3-dione (K-4): Yield 83%, mp 74–78 °C. ^{1}H NMR (d_6-DMSO, 500 MHz, δ, TMS = 0): 4.15 (s, 2H, -CH_2-), 4.70 (s, 2H, -CH_2-), 5.34 (s, 2H, -CH_2-), 6.10 (s, 1H, -CH-), 6.84 (d, 1H, J = 8 Hz, ArH), 7.37–7.41 (m, 2H, ArH), 7.65–7.71 (m, 4H, ArH), 8.44 (s, 1H, ArH). ^{13}C NMR (d_6-DMSO, 125 MHz, δ, TMS = 0): 47.55, 63.15, 91.69, 112.80, 115.52, 116.92, 119.52, 123.26, 124.71, 126.56, 127.24, 133.29, 140.17, 149.57, 153.21, 155.86, 162.02, 164.77, 182.12. Anal. Calcd for $C_{22}H_{15}BrN_4O_5$: C, 53.35; H, 3.05; Br, 16.13; N, 11.31 Found: C, 53.44; H, 3.01; Br, 16.33; N, 11.12.

1-(2-(4-((2-oxo-2H-chromen-4-yloxy)methyl)-1H-1,2,3-triazol-1-yl)ethyl)-5-iodoindoline-2,3-dione (K-5): Yield 81%, mp 88–91 °C. ^{1}H NMR (d_6-DMSO, 500 MHz, δ, TMS = 0): 4.17 (s, 2H, -CH_2-), 4.68 (s, 2H, -CH_2-), 5.37 (s, 2H, -CH_2-), 6.08 (s, 1H, -CH-), 6.82 (d, 1H, J = 8 Hz, ArH), 7.35–7.39 (m, 2H, ArH), 7.63–7.65 (m, 2H, ArH), 7.84–7.87 (m, 2H, ArH), 8.61 (s, 1H, ArH). ^{13}C NMR (d_6-DMSO, 125 MHz, δ, TMS = 0): 47.59, 63.23, 91.74, 112.86, 115.57, 116.91, 119.59, 123.24, 124.70, 126.53, 127.30, 133.34, 140.19, 149.52, 153.27, 155.90, 161.97, 164.73, 182.53. Anal.Calcd for $C_{22}H_{15}IN_4O_5$: C, 48.73; H, 2.79; I, 23.40; N, 10.33 Found: C, 48.93; H, 2.68; I, 23.44; N, 10.22.

1-(2-(4-((2-oxo-2H-chromen-4-yloxy)methyl)-1H-1,2,3-triazol-1-yl)ethyl)-5-nitroindoline-2,3-dione (K-6): Yield 83%, mp 104–108 °C. ^{1}H NMR (d_6-DMSO, 500 MHz, δ, TMS = 0): 4.14 (s, 2H, -CH_2-), 4.65 (s, 2H, -CH_2-), 5.37 (s, 2H, -CH_2-), 6.11 (s, 1H, -CH-), 6.83 (s, 1H, ArH), 7.41–7.44 (m, 2H, ArH), 7.61–7.64 (m, 2H, ArH), 7.96–7.99 (m, 2H, ArH), 8.76 (s, 1H, ArH). ^{13}C NMR (d_6-DMSO, 125 MHz, δ, TMS = 0): 47.71, 63.32, 91.65, 112.82, 115.55, 116.96, 119.62, 123.43, 124.76, 126.52, 127.13, 135.33, 146.56, 152.43, 153.86, 155.95, 162.45, 164.78, 182.72. Anal. Calcd for $C_{22}H_{15}N_5O_7$: C, 57.27; H, 3.28; N, 15.18Found: C, 57.42; H, 3.13; N, 15.45.

1-(2-(4-((2-oxo-2H-chromen-4-yloxy)methyl)-1H-1,2,3-triazol-1-yl)ethyl)-5-methoxyindoline-2,3-dione (K-7): Yield 75%, mp 70–74 °C. ^{1}H NMR (d_6-DMSO, 300 MHz, δ, TMS = 0): 3.68 (s, 3H, -OCH_3), 4.12 (s, 2H, -CH_2-), 4.69 (s, 2H, -CH_2-), 5.32 (s, 2H, -CH_2-), 6.06 (s, 1H, -CH-), 6.80 (d, 1H, J = 8.0 Hz, ArH), 7.07–7.09 (m, 2H, ArH), 7.33–7.39 (m, 2H, ArH), 7.63–7.66 (m, 2H, ArH), 8.42 (s, 1H, ArH). ^{13}C NMR (d_6-DMSO, 125 MHz, δ, TMS = 0): 47.61, 56.24, 63.06, 91.57, 109.50, 111.73, 112.08, 115.45, 116.87, 118.19, 123.26, 124.44, 124.64, 126.59, 133.30, 144.45, 153.67, 156.15, 158.61, 162.08, 164.77, 183.56. Anal.Calcd for $C_{23}H_{18}N_4O_6$: C, 61.88; H, 4.06; N, 12.55 Found: C, 60.99; H, 4.23; N, 12.32.

1-(3-(4-((2-oxo-2H-chromen-4-yloxy)methyl)-1H-1,2,3-triazol-1-yl)propyl)indoline-2,3-dione (L-1): Yield 76%, mp 122–125 °C. ^{1}H NMR (d_6-DMSO, 300 MHz, δ, TMS = 0): 2.23 (s, 2H, -CH_2-), 3.75 (s, 2H, -CH_2-), 4.52 (s, 2H, -CH_2-), 5.41 (s, 2H, -CH_2-), 6.15 (s, 1H, -CH-), 7.11–7.18 (m, 2H, ArH), 7.32–7.41 (m, 2H, ArH), 7.54–7.75 (m, 4H, ArH), 8.37 (s, 1H, ArH). ^{13}C NMR (d_6-DMSO, 125 MHz, δ, TMS = 0): 28.00, 37.36, 47.71, 63.29, 91.78, 110.97, 115.54, 116.94, 118.19, 123.25, 123.61, 124.70, 124.89, 125.81, 133.31, 138.45, 150.84, 153.23, 158.82, 162.03, 164.82, 183.74. Anal.Calcd for $C_{23}H_{18}N_4O_5$: C, 64.18; H, 4.22; N, 13.02 Found: C, 64.33; H, 4.11; N, 13.41.

1-(3-(4-((2-oxo-2H-chromen-4-yloxy)methyl)-1H-1,2,3-triazol-1-yl)propyl)-5-fluoroindoline-2,3-dione (L-2): Yield 79%, mp 94–97 °C. ^{1}H NMR (d_6-DMSO, 300 MHz, δ, TMS = 0): 2.18 (s, 2H, -CH_2-), 4.19 (s, 2H, -CH_2-), 4.77 (s, 2H, -CH_2-), 5.37 (s, 2H, -CH_2-), 6.15 (s, 1H, -CH-), 6.93

(s, 1H, ArH), 7.43–7.48 (m, 4H, ArH), 7.70–7.74 (m, 2H, ArH), 8.50 (s, 1H, ArH). ^{13}C NMR (d_6-DMSO, 125 MHz, δ, TMS = 0): 28.87, 47.56, 63.21, 79.32, 79.31, 79.54, 91.66, 111.83, 112.12, 112.21, 115.43, 116.82, 118.52, 118.59, 123.32, 124.64, 133.19, 146.82, 153.14, 158.73, 162.23, 164.69, 183.74. Anal.Calcd for $C_{23}H_{17}FN_4O_5$: C, 61.61; H, 3.82; F, 4.24; N, 12.49 Found: C, 61.45; H, 3.95; F, 4.06; N, 12.53.

1-(3-(4-((2-oxo-2H-chromen-4-yloxy)methyl)-1H-1,2,3-triazol-1-yl)propyl)-5-chloroindoline-2,3-dione (L-3): Yield 71%, mp 166–169 °C. ^{1}H NMR (d_6-DMSO, 500 MHz, δ, TMS = 0): 2.20 (s, 2H, -CH_2-), 3.74 (s, 2H, -CH_2-), 4.51 (s, 2H, -CH_2-), 5.41 (s, 2H, -CH_2-), 6.15 (s, 1H, -CH-), 7.03–7.04 (m, 1H, ArH), 7.34–7.41 (m, 2H), 7.66–7.96 (m, 4H, ArH), 8.35 (s, 1H, ArH). ^{13}C NMR (d_6-DMSO, 125 MHz, δ, TMS = 0): 27.87, 37.40, 47.65, 63.30, 86.47, 91.78, 113.48, 115.54, 116.95, 123.35, 124.70, 125.76, 132.53, 133.32, 145.86, 150.17, 153.23, 158.17, 162.03, 164.83, 182.41. Anal.Calcd for $C_{23}H_{17}ClN_4O_5$: C, 59.43; H, 3.69; Cl, 7.63; N, 12.05 Found: C, 59.60; H, 3.55; Cl, 7.75; N, 12.01.

1-(3-(4-((2-oxo-2H-chromen-4-yloxy)methyl)-1H-1,2,3-triazol-1-yl)propyl)-5-bromoindoline-2,3-dione (L-4): Yield 80%, mp 74–78 °C. ^{1}H NMR (d_6-DMSO, 500 MHz, δ, TMS = 0): 2.16 (s, 2H, -CH_2-), 4.17 (s, 2H, -CH_2-), 4.72 (s, 2H, -CH_2-), 5.35 (s, 2H, -CH_2-), 6.08 (s, 1H, -CH-), 6.86 (d, 1H, J = 8 Hz, ArH), 7.38–7.42 (m, 2H, ArH), 7.64–7.70 (m, 4H, ArH), 8.46 (s, 1H, ArH). ^{13}C NMR (d_6-DMSO, 125 MHz, δ, TMS = 0): 28.66, 47.59, 63.12, 91.71, 112.89, 115.56, 116.97, 119.57, 123.29, 124.76, 126.58, 127.28, 133.32, 140.19, 149.59, 153.28, 155.89, 162.06, 164.79, 182.56. Anal.Calcd for $C_{23}H_{17}BrN_4O_5$: C, 54.24; H, 3.36; Br, 15.69; N, 11.00 Found: C, 54.28; H, 3.15; Br, 15.78; N, 11.03.

1-(3-(4-((2-oxo-2H-chromen-4-yloxy)methyl)-1H-1,2,3-triazol-1-yl)propyl)-5-iodoindoline-2,3-dione (L-5): Yield 83%, mp 98–102 °C. ^{1}H NMR (d_6-DMSO, 500 MHz, δ, TMS = 0): 2.13 (s, 2H, -CH_2-), 4.14 (s, 2H, -CH_2-), 4.70 (s, 2H, -CH_2-), 5.35 (s, 2H, -CH_2-), 6.11 (s, 1H, -CH-), 6.81 (s, 1H, ArH), 7.36–7.39 (m, 2H, ArH), 7.65–7.68 (m, 2H, ArH), 7.80–7.84 (m, 2H, ArH), 8.59 (s, 1H, ArH). ^{13}C NMR (d_6-DMSO, 125 MHz, δ, TMS = 0): 28.69, 47.65, 63.28, 91.72, 112.81, 115.54, 116.98, 119.63, 123.23, 124.72, 126.57, 127.33, 133.37, 140.14, 149.56, 153.24, 155.94, 161.94, 164.76, 182.63. Anal.Calcd for $C_{23}H_{17}IN_4O_5$: C, 49.66; H, 3.08; I, 22.81; N, 10.07 Found: C, 49.55; H, 2.88; I, 22.84; N, 10.01.

1-(3-(4-((2-oxo-2H-chromen-4-yloxy)methyl)-1H-1,2,3-triazol-1-yl)propyl)-5-nitroindoline-2,3-dione (L-6): Yield 79%, mp 106–109 °C. ^{1}H NMR (d_6-DMSO, 500 MHz, δ, TMS = 0): 2.14 (s, 2H, -CH_2-), 4.15 (s, 2H, -CH_2-), 4.65 (s, 2H, -CH_2-), 5.34 (s, 2H, -CH_2-), 6.10 (s, 1H, -CH-), 6.83 (s, 1H, ArH), 7.42–7.45 (m, 2H, ArH), 7.61–7.67 (m, 3H, ArH), 7.97–7.99 (m, 1H, ArH), 8.76 (s, 1H, ArH). ^{13}C NMR (d_6-DMSO, 125 MHz, δ, TMS = 0): 28.56, 47.73, 63.31, 91.64, 112.83, 115.56, 116.92, 119.65, 123.43, 124.77, 126.52, 127.16, 135.34, 146.53, 152.46, 153.82, 155.94, 162.55, 164.74, 182.72. Anal.Calcd for $C_{23}H_{17}N_5O_7$: C, 58.11; H, 3.60; N, 14.73Found:C, 58.19; H, 3.51; N, 14.99.

1-(3-(4-((2-oxo-2H-chromen-4-yloxy)methyl)-1H-1,2,3-triazol-1-yl)propyl)-5-methoxyindoline-2,3-dione (L-7): Yield 76%, mp 87–90 °C. ^{1}H NMR (d_6-DMSO, 300 MHz, δ, TMS = 0): 2.19–2.24 (m, 2H, -CH_2-), 3.71–3.76 (m, 3H, -OCH_3), 4.50–4.53 (m, 2H, -CH_2-), 5.41 (s, 2H, -CH_2-), 6.15 (s, 1H, -CH-), 7.10–7.14 (m, 2H, ArH), 7.21–7.23 (m, 1H, ArH), 7.32–7.41 (m, 2H, ArH), 7.64–07.75 (m, 2H, ArH), 8.37 (s, 1H, ArH). ^{13}C NMR (d_6-DMSO, 125 MHz, δ, TMS = 0): 27.99, 36.26, 37.34, 47.71, 56.36, 63.30, 91.77, 109.76, 112.04, 115.54, 116.93, 118.68, 123.35, 124.09, 124.69, 133.31, 144.59, 153.22, 156.16, 158.82, 162.03, 164.83, 183.98. Anal.Calcd for $C_{24}H_{20}N_4O_6$: C, 62.60; H, 4.38; N, 12.17 Found: C, 62.66; H, 4.13; N, 12.34.

1-(4-(4-((2-oxo-2H-chromen-4-yloxy)methyl)-1H-1,2,3-triazol-1-yl)butyl)indoline-2,3-dione(M-1): Yield 74%, mp 146–150 °C. ^{1}H NMR (d_6-DMSO, 500 MHz, δ, TMS = 0): 1.58–1.61 (m, 2H, -CH_2-), 1.92–1.95 (m, 2H, -CH_2-), 3.69–3.72 (m, 2H, -CH_2-), 4.44–4.47 (m, 2H, -CH_2-), 5.40 (s, 2H, -CH_2-), 6.14 (s, 1H, -CH-), 7.11–7.18 (m, 2H, ArH), 7.34–7.41 (m, 2H, ArH), 7.53 (d, 1H, J = 7 Hz, ArH), 7.63–7.66 (m, 2H, ArH), 7.73 (d, 1H, J = 7.5 Hz, ArH), 8.38 (s, 1H, ArH). ^{13}C NMR (d_6-DMSO, 125 MHz, δ, TMS = 0): 24.25, 27.42, 49.53, 63.33, 91.77, 111.06, 115.54, 116.91, 118.01, 123.33, 123.58, 124.66, 124.90, 133.26, 138.51, 151.03, 153.22, 158.67, 161.98, 164.81, 183.86. Anal.Calcd for $C_{24}H_{20}N_4O_5$: C, 64.86; H, 4.54; N, 12.61 Found: C, 64.97; H, 4.32; N, 12.85.

1-(4-(4-((2-oxo-2H-chromen-4-yloxy)methyl)-1H-1,2,3-triazol-1-yl)butyl)-5-fluoroindoline-2,3-dione (M-2): Yield 77%, mp 110–114 °C. ^{1}H NMR (d_6-DMSO, 300 MHz, δ, TMS = 0): 1.59 (s, 2H, -CH_2-), 1.87 (s, 2H, -CH_2-), 3.70 (s, 2H, -CH_2-), 4.44 (s, 2H, -CH_2-), 5.34 (s, 2H, -CH_2-), 6.13 (s, 1H, -CH_2-), 6.91 (s, 1H, -CH-), 7.44–7.49 (m, 4H, ArH), 7.72–7.74 (m, 2H, ArH), 8.52 (s, 1H, ArH). ^{13}C NMR (d_6-DMSO, 125 MHz, δ, TMS = 0): 24.44, 27.34, 47.52, 63.25, 79.32, 79.38, 79.53, 91.65, 111.83, 112.11, 112.29, 115.42, 116.81, 118.55, 118.68, 123.32, 124.61, 133.23, 146.81, 153.15, 158.77, 162.19, 164.71, 183.72. Anal.Calcd for $C_{24}H_{19}FN_4O_5$: C, 62.34; H, 4.14; F, 4.11; N, 12.12 Found: C, 62.62; H, 4.25; F, 3.99; N, 12.19.

1-(4-(4-((2-oxo-2H-chromen-4-yloxy)methyl)-1H-1,2,3-triazol-1-yl)butyl)-5-chloroindoline-2,3-dione (M-3): Yield 70%, mp 170–172 °C. ^{1}H NMR (d_6-DMSO, 500 MHz, δ, TMS = 0): 1.56 (s, 2H, -CH_2-), 1.92 (s, 2H, -CH_2-), 3.68 (s, 2H, -CH_2-), 4.44 (s, 2H, -CH_2-), 5.39 (s, 2H, -CH_2-), 6.13 (s, 1H, -CH-), 7.20–7.40 (m, 3H, ArH), 7.56–7.73 (m, 4H, ArH), 8.39 (s, 1H, ArH). ^{13}C NMR (d_6-DMSO, 125 MHz, δ, TMS = 0): 24.14, 27.30, 49.56, 63.37, 91.75, 112.75, 115.52, 116.89, 119.43, 123.33, 124.37, 124.67, 127.79, 133.27, 137.29, 149.53, 153.20, 158.46, 162.01, 164.82, 182.75. Anal.Calcd for $C_{24}H_{19}ClN_4O_5$: C, 60.19; H, 4.00; Cl, 7.40; N, 11.70 Found: C, 60.30; H, 3.88; Cl, 7.47; N, 11.64.

1-(4-(4-((2-oxo-2H-chromen-4-yloxy)methyl)-1H-1,2,3-triazol-1-yl)butyl)-5-bromoindoline-2,3-dione (M-4): Yield 76%, mp 75–80 °C. ^{1}H NMR (d_6-DMSO, 500 MHz, δ, TMS = 0): 1.57 (s, 2H, -CH_2-), 1.92 (s, 2H, -CH_2-), 3.69 (s, 2H, -CH_2-), 4.44 (s, 2H, -CH_2-), 5.40 (s, 2H, -CH_2-), 6.14 (s, 1H, -CH-), 7.16 (s, 1H, ArH), 7.34–7.41 (m, 2H, ArH), 7.66–7.80 (m, 4H, ArH), 8.38 (s, 1H, ArH). ^{13}C NMR (d_6-DMSO, 125 MHz, δ, TMS = 0): 24.13, 27.31, 49.55, 63.36, 88.90, 91.77, 113.20, 115.27, 115.53, 116.91, 119.83, 123.34, 124.46, 127.10, 133.27, 140.09, 147.92, 153.21, 158.30, 161.99, 164.81, 182.61. Anal.Calcd for $C_{24}H_{19}BrN_4O_5$: C, 55.08; H, 3.66; Br, 15.27; N, 10.71 Found: C, 55.25; H, 3.44; Br, 15.45; N, 10.55.

1-(4-(4-((2-oxo-2H-chromen-4-yloxy)methyl)-1H-1,2,3-triazol-1-yl)butyl)-5-iodoindoline-2,3-dione (M-5): Yield 83%, mp 97–102 °C. ^{1}H NMR (d_6-DMSO, 500 MHz, δ, TMS = 0): 1.58 (s, 2H, -CH_2-), 1.91 (s, 2H, -CH_2-), 3.71 (s, 2H, -CH_2-), 4.44 (s, 2H, -CH_2-), 5.38 (s, 2H, -CH_2-), 6.08 (s, 1H, -CH-), 6.84 (s, 1H, ArH), 7.34–7.37 (m, 2H, ArH), 7.67–7.69 (m, 2H, ArH), 7.76–7.79 (m, 2H, ArH), 8.61 (s, 1H, ArH). ^{13}C NMR (d_6-DMSO, 125 MHz, δ, TMS = 0): 24.54, 27.43, 48.99, 63.56, 91.76, 112.82, 115.58, 117.12, 119.67, 123.25, 124.77, 126.53, 127.33, 133.32, 140.11, 149.45, 153.00, 155.95, 161.94, 164.71, 182.73. Anal. Calcd for $C_{24}H_{19}IN_4O_5$: C, 50.54; H, 3.36; I, 22.25; N, 9.82 Found: C, 50.51; H, 3.45; I, 22.12; N, 10.00.

1-(4-(4-((2-oxo-2H-chromen-4-yloxy)methyl)-1H-1,2,3-triazol-1-yl)butyl)-5-nitroindoline-2,3-dione (M-6): Yield 80%, mp 110–112 °C. ^{1}H NMR (d_6-DMSO, 500 MHz, δ, TMS = 0): 1.57 (s, 2H, -CH_2-), 1.92 (s, 2H, -CH_2-), 3.66 (s, 2H, -CH_2-), 4.43 (s, 2H, -CH_2-), 5.37 (s, 2H, -CH_2-), 6.10 (s, 1H, -CH-), 6.84 (s, 1H, ArH), 7.44–7.47 (m, 2H, ArH), 7.62–7.67 (m, 2H, ArH), 7.94–7.96 (m, 2H, ArH), 8.72 (s, 1H, ArH). ^{13}C NMR (d_6-DMSO, 125 MHz, δ, TMS = 0): 24.34, 27.65, 48.56, 63.65, 91.34, 112.87, 115.52, 116.97, 119.63, 123.46, 124.73, 126.55, 127.12, 135.35, 146.56, 152.43, 153.84, 155.96, 162.53, 164.77, 182.69. Anal. Calcd for $C_{24}H_{19}N_5O_7$: C, 58.90; H, 3.91; N, 14.31 Found: C, 58.99; H, 3.76; N, 14.42.

1-(4-(4-((2-oxo-2H-chromen-4-yloxy)methyl)-1H-1,2,3-triazol-1-yl)butyl)-5-methoxyindoline-2,3-dione (M-7): Yield 73%, mp 97–100 °C. ^{1}H NMR (d_6-DMSO, 300 MHz, δ, TMS = 0): 1.57 (s, 2H, -CH_2-), 1.92 (s, 2H, -CH_2-), 3.67 (s, 2H, -CH_2-), 3.75 (s, 3H, -OCH_3), 4.44 (s, 2H, -CH_2-), 5.39 (s, 2H, -CH_2-), 6.13 (s, 1H, -CH-), 7.09–7.11 (m, 2H, ArH), 7.20–7.22 (m, 1H, ArH), 7.33–7.35 (m, 1H, ArH), 7.39–7.40 (m, 1H, ArH), 7.65–7.67 (m, 1H, ArH), 7.72–7.73 (m, 1H, ArH), 8.37 (s, 1H, ArH). ^{13}C NMR (d_6-DMSO, 125 MHz, δ, TMS = 0): 24.23, 27.39, 49.53, 56.35, 63.32, 91.74, 109.78, 112.13, 115.52, 116.90, 118.18, 123.33, 124.23, 124.68, 125.58, 133.28, 144.78, 153.20, 156.14, 158.67, 162.02, 164.83, 184.12. Anal.Calcd for $C_{25}H_{22}N_4O_6$: C, 63.29; H, 4.67; N, 11.81 Found: C, 63.45; H, 4.47; N, 11.92.

In vitro xanthine oxidase assay

All the synthesized compounds were evaluated against XO enzyme. Bovine milk XO (grade 1, ammonium sulfate suspension, Sigma-Aldrich, India) activity was assayed spectrophotometrically by measuring the UA formation at 293 nm using a Hitachi U-3010 UV-visible spectrophotometer at 25 °C. The reaction mixture contains 50 mM potassium phosphate buffer (pH 7.6), 75 μM xanthine, and 0.08 units of XO. Inhibition of XO activity of synthetics at different concentrations (1, 5, 10, 25, 50 μM) was measured by following the decrease in the UA formation at 293 nm at 25 °C. The enzyme was pre-incubated for 5 min with a test compound, dissolved in DMSO (1% v/v), and the reaction was started by the addition of xanthine. The final concentration of DMSO (1% v/v) did not interfere with the enzyme activity. All the experiments were performed in triplicate and values were expressed as the mean of three experiments (Escribano et al. 1988; Takano et al. 2005).

Enzyme kinetics study

Potent XO enzyme inhibitors were further investigated for the type of inhibition and enzyme kinetics study was carried out. The Lineweaver–Burk plot was established from which we could calculate the K_m, V_{max} of the slope of inhibitor and the value of α (a constant that defines the degree to which inhibitor binding affects the affinity of the enzyme for substrate (Copeland 2005).

Molecular modeling studies

Crystal structure of XO (PDB entry: 1N5X; resolution 2.8 Å) was downloaded from Protein Data Bank.

Preparation of structure was done by using drug design platform LeadIT. Co-crystalized ligand Febuxostat was used for defining binding site with the radius of 6.50 Å. Structure of compound was drawn on ChemDraw Ultra (2013) and its energy was minimized by employing MM2 force field in Chem 3D Ultra software. Prepared compound was used as protonated in aqueous solution and docked into prepared binding site using FlexX docking module in LeadIT. All FlexX solutions obtained were scored using a consensus scoring function (CScore) and ranked accordingly. Top best pose with the highest score was selected for investigation of interactions. 3D enzyme-hybrid interactions were visualized using Discovery Studio Visualizer: Biovia 2016.

Acknowledgements Authors are grateful to the University Grants Commission for providing funds under Rajiv Gandhi National Fellowship (RGNF) and National Fellowships for Other Backword Classes (NFOBC), Department of Science & Technology (DST-PURSE), Council of Scientific and Industrial Research (CSIR): Project no. 02(0319)17/EMR-II, Women Scientists Scheme-A (WOS-A: DST) and DST-FIST. The authors are also thankful to Guru Nanak Dev University, Amritsar for providing various basic facilities to carry out the research work.

Compliance with ethical standards

Conflict of interest The authors declare that they have no conflict of interest.

Publisher's note Springer Nature remains neutral with regard to jurisdictional claims in published maps and institutional affiliations.

References

Ali HI, Fujita T, Akaho E, Nagamatsu T (2010) A comparative study of AutoDock and PMF scoring performances, and SAR of 2-substituted pyrazolotriazolopyrimidines and 4-substituted pyrazolopyrimidines as potent xanthine oxidase inhibitors. J Comput Aided Mol Des 24:57–75

Becker MA, Kisicki J, Khosravan R, Wu J, Mulford D, Hunt B, MacDonald P, Joseph-Ridge N (2004) Febuxostat (TMX-67), a novel, non-purine, selective inhibitor of xanthine oxidase, is safe and decreases serum urate in healthy volunteers. Nucl Nucl Nucl 23:35–40

Becker M, Schumacher H, MacDonald PA (2007) Febuxostat: a guide to its use in chronic hyperuricaemia. Abstr no 757 Arthritis Rheum 56(9 Suppl):S322

Biagi G, Giorgi I, Pacchini F, Livi O, Scartoni V (2001) 2-Alkyloxyalkylthiohypoxanthines as new potent inhibitors of xanthine oxidase. Farmaco 56:809–813

Borges F, Fernandes E, Roleira F (2002) Progress towards the discovery of xanthine oxidase inhibitors. Curr Med Chem 9:195–217

Brien DE, Springer RH, Albert TNA, Senga K, Miller JP, Streeter DG (1985) Purine analog inhibitors of xanthine oxidase - structure activity relationships and proposed binding of the molybdenum cofactor. J Heterocycl Chem 22:601–634

ChemDraw Ultra 6.0 and Chem3D Ultra (2013); Cambridge Soft Corporation: Cambridge, USA

Chen C, Huang C, Tsai K, Huang W, Huang W, Hsu Y, Hsu F (2014) Evaluation of the antihyperuricemic activity of phytochemicals from davallia formosana by enzyme assay and hyperuricemic mice model. Evid Based Complement Alternat Med 2014:1–8

Copeland RA (2005) Evaluation of Enzyme Inhibitors in Drug Discovery. Wiley, Hoboken

Dassault Systemes BIOVIA (2016) Discovery studio modeling environment, release 2017. Dassault Systemes, San Diego

Dhiman R, Sharma S, Singh G, Nepali K, Bedi PMS (2012) Design and synthesis of aza-flavones as a new class of xanthine oxidase inhibitors. Arch Pharm Chem Life Sci 346:7–16

Escribano J, Gracia-Canovas F, Garcia-Carmona F (1988) A kinetic study of hypoxanthine oxidation by milk xanthine oxidase. Bio Chem J 254:829–833

Fais A, Era B, Asthana S, Sogos V, Medda R, Santana L, Uriarte E, Mtos MJ, Delogu F, Kumar A (2018) Coumarin derivatives as promising xanthine oxidase inhibitors. Ijbiomac 120:1286–1293

Hille R (2006) Structure and function of xanthine oxidoreductase. Eur J Inorg Chem 10:1913–1926

Ishibuchi S, Morimoto H, Oe T, Ikebe T, Inoue H, Fukunari A, Kamezawa M, Yamada I, Naka Y (2001) Synthesis and structure–activity relationships of 1-Phenylpyrazoles as xanthine oxidase inhibitors. Bioorg Med Chem Lett 11:879–882

Kaur C, Dhiman S, Singh H, Kaur M, Bhagat S, Gupta M, Sharma S, Bedi PMS (2015) Synthesis, screening and docking studies of benzochromone derivatives as xanthine oxidase inhibitors. J Chem Phar Res 7:127–136

Kaur G, Singh JV, Gupta MK, Bhagat K, Gulati HK, Singh A, Bedi PMS, Singh H, Sharma S (2019) Thiazole-5-carboxylic acid derivatives as potent xanthine oxidase inhibitors: design, synthesis, *in vitro* evaluation, and molecular modeling studies. Medicinal Chem Res 29:83–93

Kaur M, Kaur A, Mankotia S, Singh H, Singh A, Singh JV, Gupta MK, Sharma S, Nepali K, Bedi PMS (2017) Synthesis, screening and docking of fused pyrano[3,2-d]pyrimidine derivatives as xanthine oxidase inhibitor. Eur J Med Chem 131:14–28

Kaur R, Naaz F, Sharma S, Mehndiratta S, Gupta MK, Bedi PMS, Nepali K (2015) Screening of a library of 4-aryl/heteroaryl-4H-fused pyrans for xanthine oxidase inhibition: synthesis, biological evaluation and docking studies. Med Chem Res 24:3334–3349

Komoriya K, Osada Y, Hasegawa M, Horiuchi H, Kondo S, Couch RC, Griffin TB (1993) Hypouricemic effect of allopurinol and the novel xanthine oxidase inhibitor TEI-6720 in chimpanzees. Eur J Pharm 250:455–460

Kumar R, Darpan, Sharma S, Singh R(2011) Xanthine oxidase inhibitors: a patent survey Expert Opin Ther Pat 21:1071–1108

Love BL, Barrons R, Veverka A, Snider KM (2010) Urate-lowering therapy for gout: focus on febuxostat. Pharmacother 30:594–608

Malik N, Dhiman P, Sobarzo-Sanchez E, Khatkar A (2018) Flavonoids and anthranquinones as xanthine oxidase and monoamine oxidase inhibitors: a new approach towards inflammation and oxidative stress. Curr Top Med Chem 18:2154–2164

Mehmood A, Ishaq M, Zhao L, Safdar B, Rehman AU, Munir M, Raza A, Nadeem M, Iqbal W, Wang C (2019) Natural compounds with xanthine oxidase inhibitory activity: a review. Chem Biol Drug Des 93:387–418

Nagamatsu T, Fujita T, Endo K (2000) Novel xanthine oxidase inhibitor studies. Part 2. Synthesis and xanthine oxidase inhibitory activities of 2-substituted 6-alkylidenehydrazino- or 6-arylmethylidenehydrazino-7H-purines and 3- and/or 5-substituted 9H-1,2,4-triazolo[3,4-i]purines. Perkin Trans 1:33–38

Nagamatsu T, Ukai M,F, Yoneda F, Brown DJ (1985) Syntheses of 4 Methyl-s-triazolo[4,3-a]purin-9(4H)-ones and tetrazolo-[1,5-a] purin-9(4H)-ones as Aza Analogs of "Y" Bases. Chem Pharm Bull 33:3113–3121

Nagamatsu T, Yamasaki H (1995) Facile, general and productive syntheses of the fluorescent wye (4,9-dihydro-4,6-dimethyl-9-oxo-1H-imidazo[1,2-a]purine) in phenylalanine tRNA, its 2-substituted derivatives and 7-aza analogues. J Chem Soc Chem Commun 19:2041–2043

Oettl K, Reibneggar G (1999) Pteridines as inhibitors of xanthine oxidase: structural requirements. Biochim Biophys Acta 1430:387–395

Ojha R, Singh J, Ojha A, Singh H, Sharma S, Nepali K (2017) An updated patent review: xanthine oxidase inhibitors for the treatment of hyperuricemia and gout (2011-2015). Expert Opin Ther Pat 27:311–345

Osada Y, Tsuchimoto M, Fukushima H, Takahashi K, Kondo S, Hasegawa M, Komoriya K (1993) Hypouricemic effect of the novel xanthine oxidase inhibitor, TEI-6720, in rodents. Eur J Pharm 241:183–188

Pacher P, Nivorozhkin A, Szabo C (2006) Therapeutic effects of xanthine oxidase inhibitors: renaissance half a century after the discovery of allopurinol. Pharm Rev 58:87–114

Pascart T, Richette P (2018) Investigational drugs for hyperuricemia, an update on recent developments. Expert Opin Inv Drug 27:437–444

Schumacher HRJ, Becker MA, Wortmann RL, Macdonald PA, Hunt B, Streit J, Lademacher C, Joseph-Ridge N (2008) Effects of febuxostat versus allopurinol and placebo in reducing serum urate in subjects with hyperuricemia and gout: a 28-week, phase III, randomized, double-blind, parallel-group trial. Arthritis Rheum 59:1540–1548

Sebastian E, Sattui, Gaffo AL (2016) Treatment of hyperuricemia in gout: current therapeutic options, latest developments and clinical implications. Ther Adv Musculoskel Dis 8:145–159

Singh JV, Mal G, Kaur G, Gupta MK, Singh A, Nepali K, Singh H, Sharma S, Bedi PMS (2019) Benzoflavone derivatives as potent antihyperuricemic agents. Med Chem Commun 10:128–147

Sharma S, Sharma K, Ojha R, Kumar D, Singh G, Nepali K, Bedi PMS (2014) Microwave assisted synthesis of naphthopyrans catalysed by silica supported fluoroboric acid as a new class of non purine xanthine oxidase inhibitors. Bioorg Med Chem Lett 24:495–500

Shukla S, Kumar D, Ojha R, Gupta MK, Nepali K, Bedi PMS (2014) 4,6-Diaryl/heteroarylpyrimidin-2(1H)-ones as a new class of xanthine oxidase inhibitors. Arch Pharm Chem Life Sci 347:1–10

Strilchuk L, Fogacci F, Cicero AF (2019) Safety and tolerability of available urate-lowering drugs: a critical review. Expert Opin Drug Saf 18:261–271

Takano Y, Hase-Aoki K, Horiuchi H, Zhao L, Kasahara Y, Kondo S, Becker MA (2005) Selectivity of febuxostat, a novel non-purine inhibitor of xanthine oxidase/xanthine dehydrogenase. Life Sci 76:1835–1847

Virdi HS, Sharma S, Mehndiratta S, Bedi PMS, Nepali K (2014) Design, synthesis and evaluation of 2,4-diarylpyrano[3,2-c] chromen-5(4H)-one as a new class of non-purine xanthine oxidase inhibitors. J Enzym Inhib Med Chem 30:1–7

Wortmann RL (1998) Gout and other disorders of purine metabolism. In: Brunwald E ed. Harrison's principles of internal medicine. McGraw-Hill, New York (NY), Vol. 14, p 2158–2166